Predicting Coastal Flooding in the Mediterranean with Remote Sensing and Machine Learning

Alice Re[1], Lorenzo Minola[1,2,3], Alessandro Pezzoli[1] and Gustau Camps-Valls[4]

[1]Interuniversity Department of Regional and Urban Studies and Planning (DIST), Politecnico and University of Turin, Turin, Italy
[2]Regional Climate Group, Department of Earth Sciences, University of Gothenburg, Gothenburg, Sweden.
[3]CIDE, CSIC-UV-Generalitat Valenciana, Climate, Atmosphere and Ocean Laboratory (Climatoc-Lab), Moncada, Valencia, Spain.
[4]Image Processing Laboratory (IPL), Universitat de València, Spain

{alice.re@polito.it}

- A **data-driven approach** to the identification of areas susceptible to coastal (and compound) flooding for the Italian region Liguria.
- **Supervised binary classification** → models of varying levels of complexity and spatial aggregation.
- An **insight into the use of Remote Sensing** (optical and SAR) within the study is presented here.

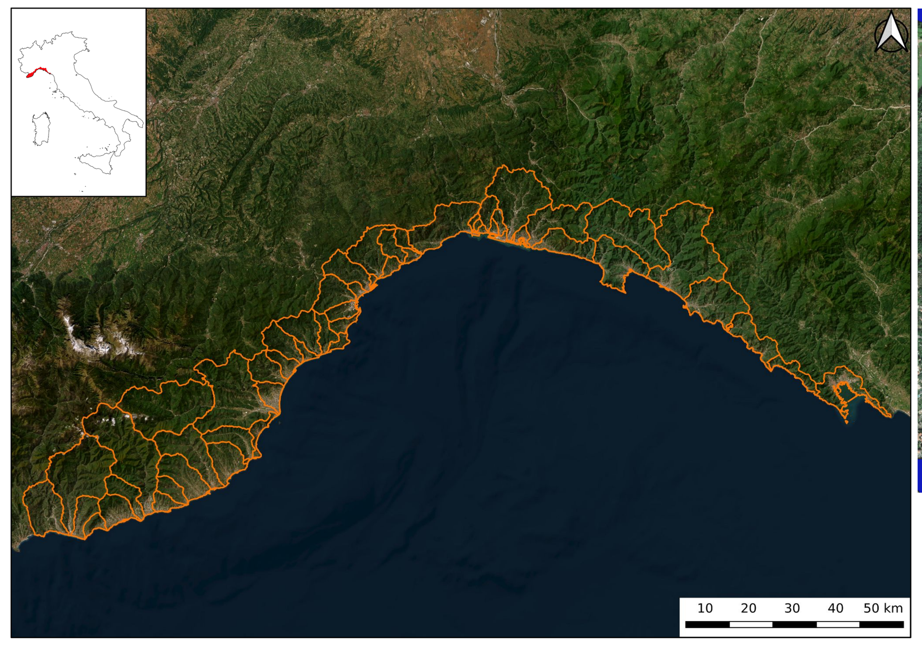

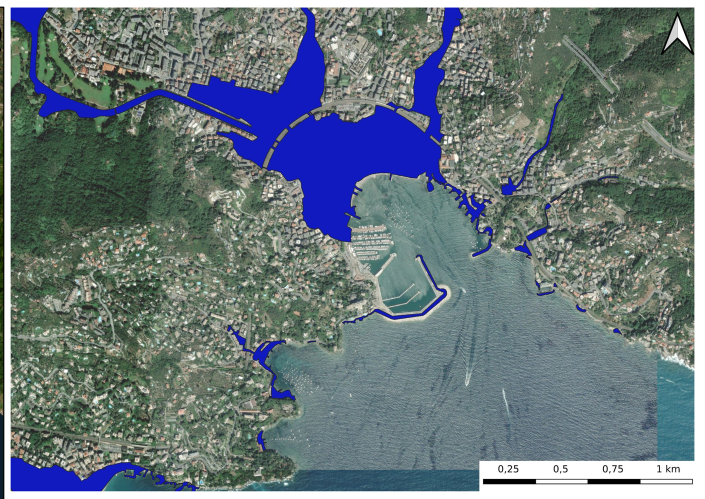

Figure 1 (left): Map of the study area and superimposed outline of individual Units of Analysis (UoAs) utilised in the study. The top-left portion of the image highlights the location of the study area (in red) within the Italian territory.
Figure 2 (above): Detail of the coastline in the Rapallo area, including the Carlo Riva port: map of the modelled ground truth data used in the study (blue vector) superimposed to optical imagery.
Base map for both images: ESRI Satellite.

Data and methods

Desired Output:

Each pixel classified as either flooded or not flooded in the event of a **medium probability flooding event** (RT = 100 yrs) (cf. **Fig. 6**).

Predictors:
- aspect
- curvature
- slope
- distance from coastline
- DEM
- DEM-derived indices: Overland Flow Distance (OFD) from channel network, its vertical (VOFD) and horizontal (HOFD) components, Vertical Distance to Channel (VDC)
- lithology
- land cover
- spectral indices: NDBI, NDVI, NDWI
- Topographic Position Index (TPI)
- Topographic Wetness Index (TWI)

Ground Truth:
- EU Floods Directive flood risk maps.
- Several modelling methodologies (numerical/simplified) used within the study area.
- Binary rasters created from maps (cf. **Fig. 2**) (0 = no flood; 1 = flood).

Modelling Matrix	Model Complexity →		
Spatial Detail ↓	Linear Classifier + All Study Area	RF Classifier + All Study Area	N.A.
	Linear Classifier + Individual UoAs	RF Classifier + Individual UoAs	Image Segmentation with CNN + some test UoAs

Comparison of model performance and computational times with known data on hydrodynamic models

Preliminary Results

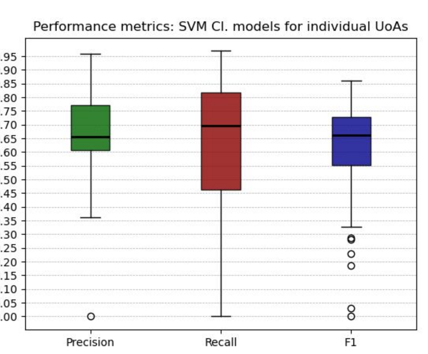

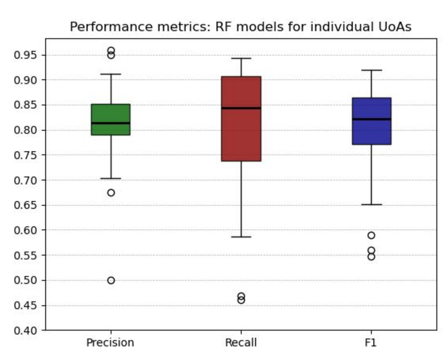

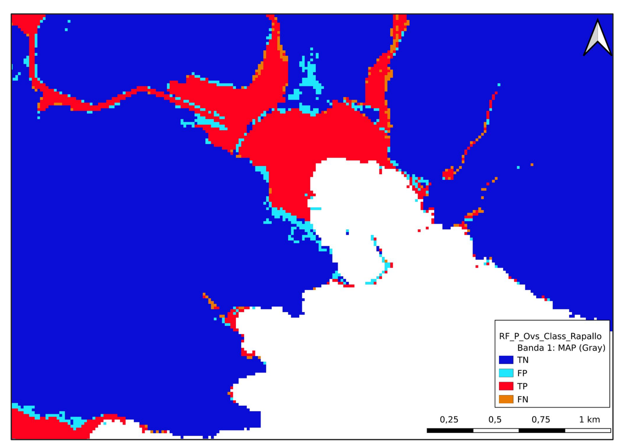

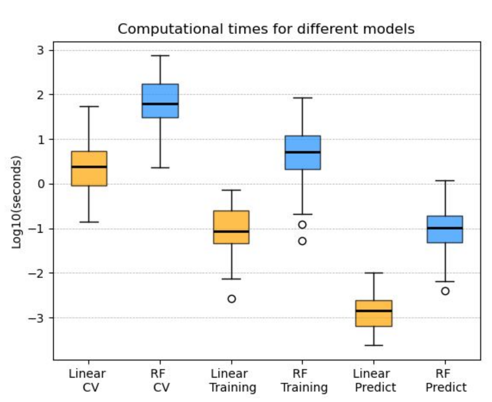

Figures 3 (upper-left) and 4 (upper-right): Boxplots of model performance metrics for linear (left) and Random Forest (right) models trained on individual Units Of Analysis (cf. **Fig. 1**).
Figure 5 (left): Boxplots of computational times for linear and RF models.

Figure 6 (above): Model Outputs obtained with the Random Forest model for the Rapallo area. Different colours are used to identify true negatives (blue), true positives (red), false positives (light blue) and false negatives (orange) produced by the model. The flooded area (TP) is the same as shown in **Fig. 2.**

Observed coastal flooding events in the area

Coastal Flooding on Oct. 29th, 2018 in Rapallo

Storm Adrian → October 29-30th, 2018 (Tempesta Vaia).

- Strong winds up to 120 km/h
- Wave heights up to 7-10 m

Impact: flooding in Rapallo and **destruction** of the Carlo Riva **port**.

Available satellite data for flooding event on Oct. 29th, 2018 in Rapallo

Sensor	Date (dd/mm/yyyy)	Status	Orbit-Polarisation	Resolution
Sentinel-1B	21/08/2018	Before flood	Ascending/VH	10 m
Sentinel-1A	22/08/2018	Before flood	Ascending/VH	10 m
Sentinel-1A	27/08/2018	Before flood	Ascending/VH	10 m
Sentinel-1B	01/11/2018	After flood	Ascending/VH	10 m
Sentinel-1A	02/11/2018	After flood	Ascending/VH	10 m
Sentinel-2A	19/10/2018	Before flood	– –	20 m
Sentinel-2B	03/11/2018	After flood	– –	20 m

Figure 7 (top): Damage suffered by the Carlo Riva port in Rapallo after the 29-30th October 2018 storm event. Picture by Parma1983 on Wikimedia Commons, licensed under CC-BY-SA-4.0.
Figure 8 (bottom): Damage on the seafront in Rapallo after the 29-30th October 2018 storm event. Picture by Dapa19 on Wikimedia Commons, licensed under CC-BY-SA-4.0.

Option 1: flooded area extent retrieval from optical imagery

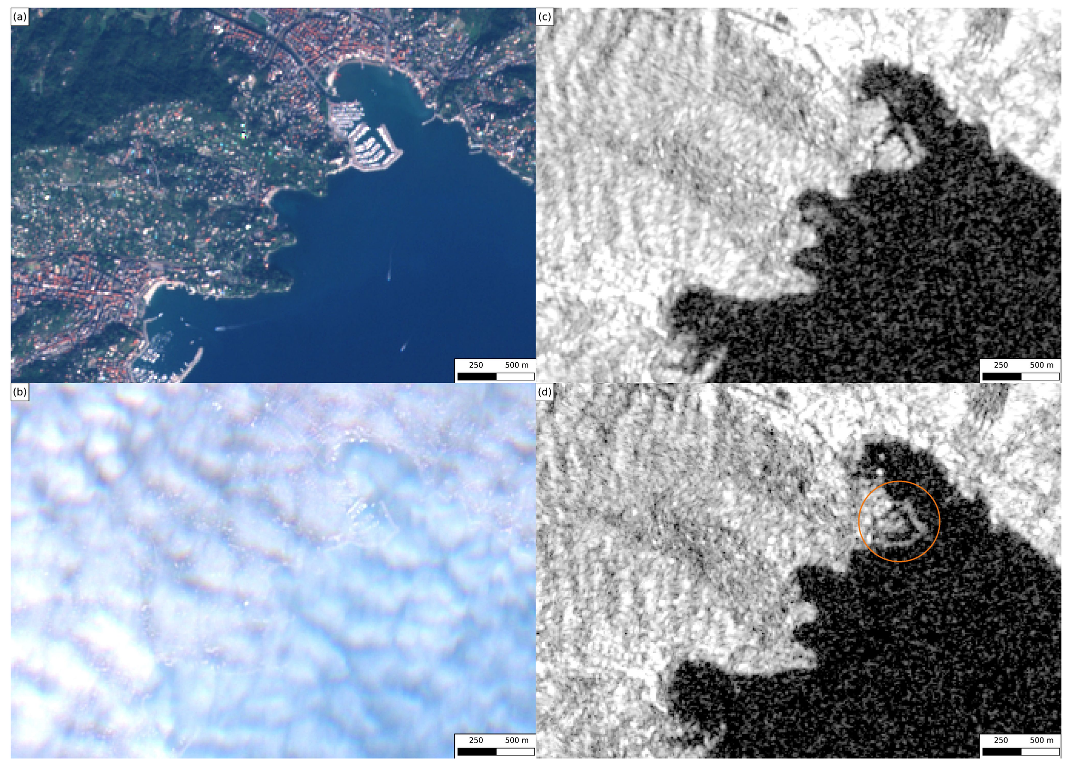

Figure 9: Optical **(a,b)** and SAR **(c,d)** satellite imagery, before **(a,c)** and after **(b,d)** the coastal flood event in Rapallo (Oct. 29th, 2018).
(a): Sentinel-2 on Oct. 16th, 2018.
(b): Sentinel-2 on Nov. 3rd, 2018.
(c): Mean of the pre-event image stack backscatter coefficient (Sentinel-1).
(d): Minimum of the post-event image stack backscatter coefficient (Sentinel-1).
The Carlo Riva port is highlighted by an orange circle in **(d)**.

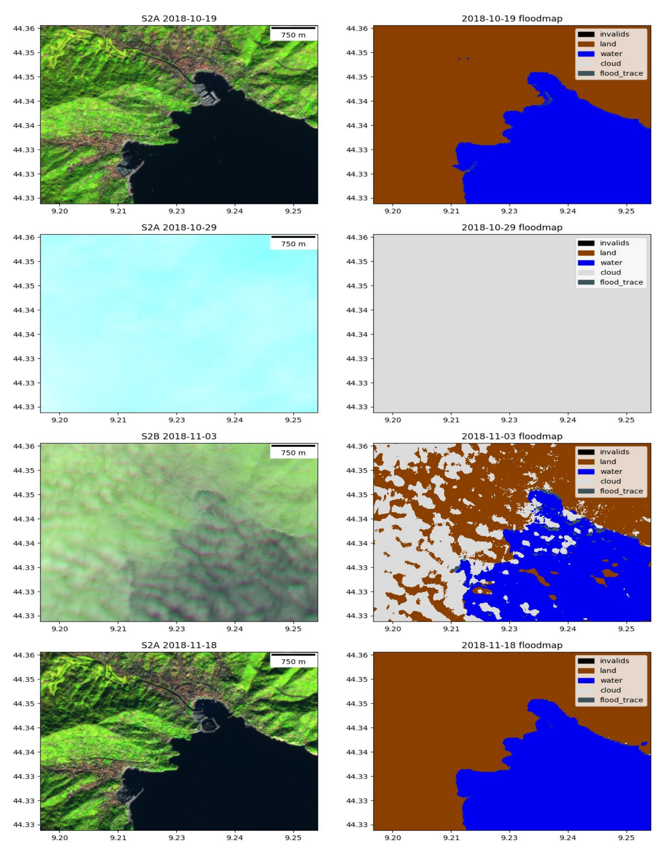

Figure 10: Optical Imagery and corresponding flood extent segmentation for the Rapallo area obtained with the ***ML4Floods*** package.

Clouds in the post-event images → ML-based image segmentation on Sentinel-2 imagery has excessive cloud cover over the area (cf. Nov. 3rd, 2018 in **Fig. 10**).

Option 2: flooded area extent retrieval from Synthetic Aperture Radar (SAR)

Three SAR **change detection-based indices** are considered.

Index thresholding for flood identification is **area-dependent** and can vary widely.

Validation by comparison with optical flood indices (e.g. MNDWI) **not** feasible in this case.

$$RI = \frac{|min(\sigma_{0[AF]})|}{|mean(\sigma_{0[BF]})|}$$

$$DII = |min(\sigma_{0[AF]})| - |mean(\sigma_{0[BF]})|$$

$$NDFI = \frac{|mean(\sigma_{0[BF]})| - |min(\sigma_{0[AF]})|}{|mean(\sigma_{0[BF]})| + |min(\sigma_{0[AF]})|}$$

Note:
$\sigma_{0[BF]}$ is the backscatter coeff. of SAR imagery before flood
$\sigma_{0[AF]}$ is the backscatter coeff. of SAR imagery after flood

SAR flood index thresholding

$$Threshold = mean(\text{SAR Index Image}) \pm k_f \times stdev(\text{SAR Index Image})$$

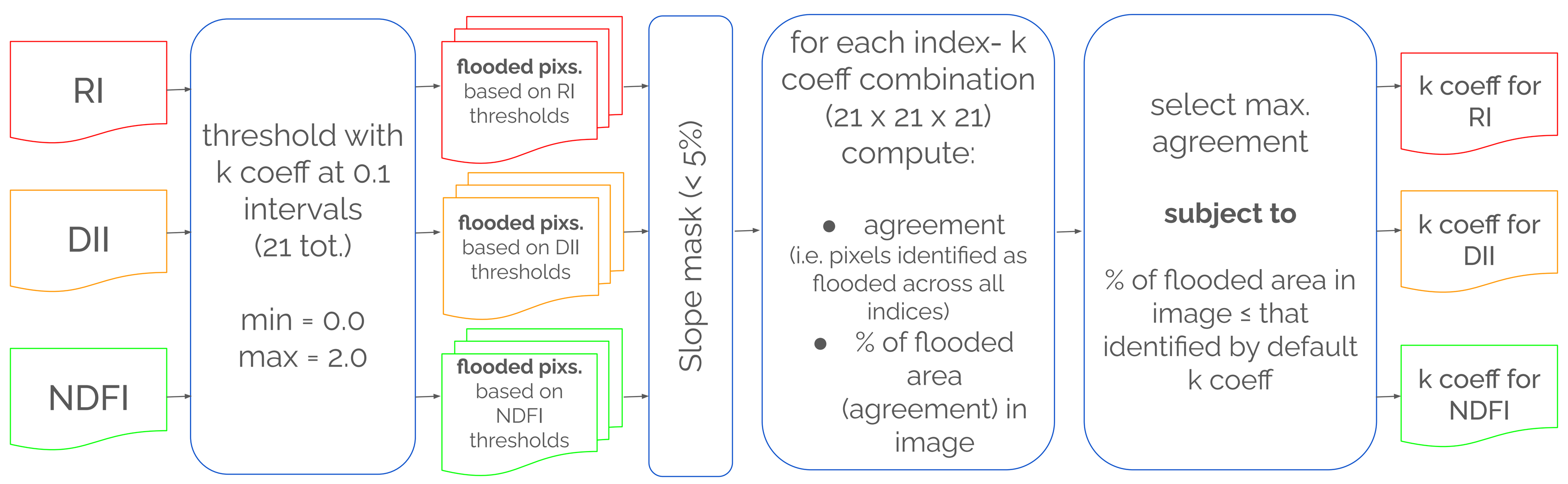

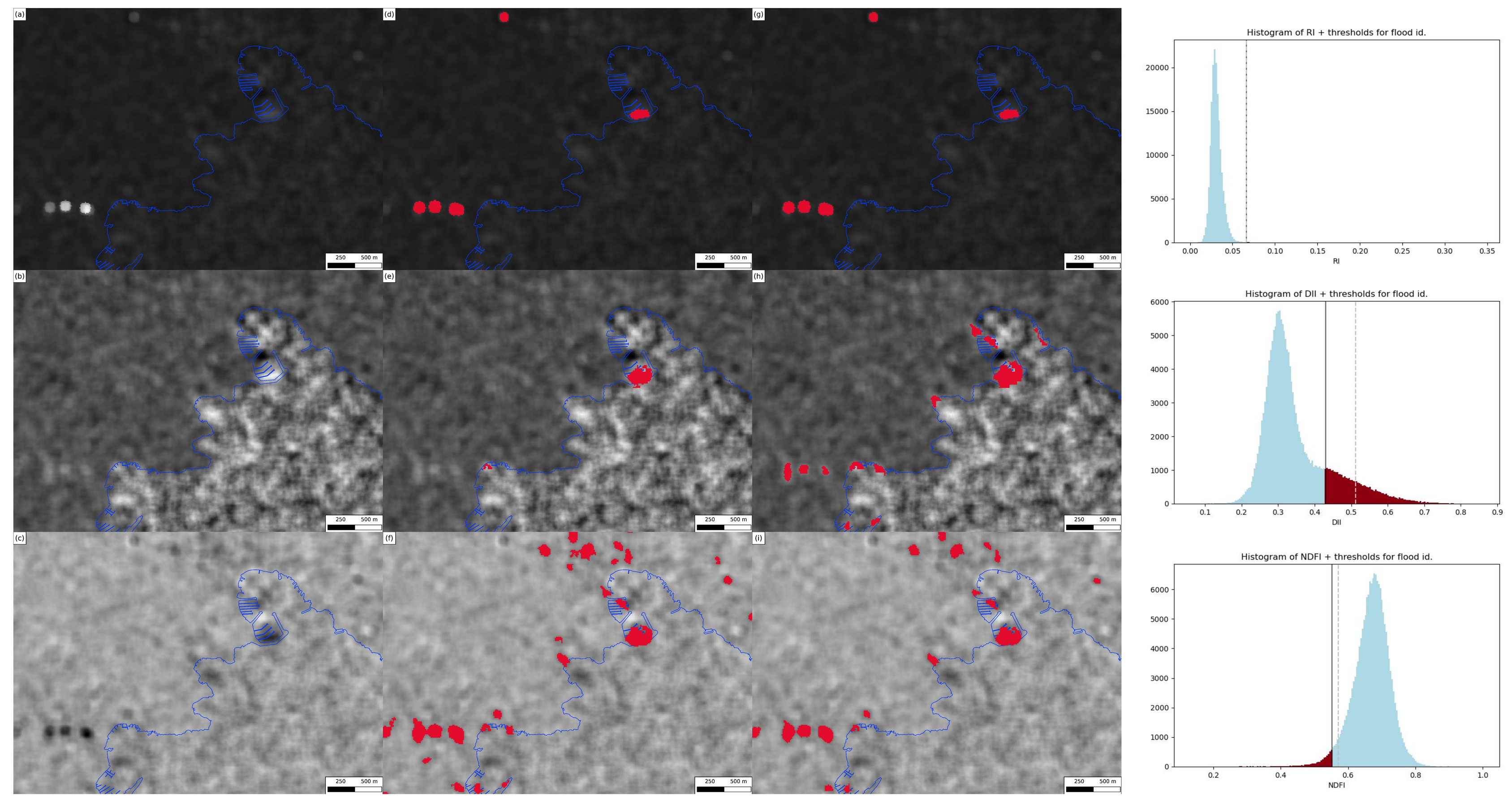

Figure 11: RII **(a)**, DII **(b)** and NDFI **(c)** for the flood event analysed (Rapallo coastline is outlined in blue in all images, including the Carlo Riva port in the upper-right area). Images **(d-e-f)** highlight in red pixels considered as flooded based on the default 1.5 k coefficient for flood thresholding, while images **(g-h-i)** are based on the k-coefficient for flood thresholding optimised for maximum agreement among the three indices. The right-hand side of the image shows histograms of the distribution of the three indices considered across all pixels included in the image, with lines corresponding to default (grey, dashed) and optimised (black, continuous) thresholds for flood identification.

Notes:
- explore **other approaches**
- **permanent water mask** → some flooded pixels lost due to image resolution
- flooded pixels **too few to serve as ground truth**

Next Steps

1. Consider model **uncertainty** and **explainability**
2. Compare model performance: **global VS local** → what are the relevant factors for flood susceptibility locally?
3. Compare model performance: **less complex VS more complex models** → are performance improvements worth the increased complexity?

References:
Camps-Valls, G., *et al.*, eds. Deep learning for the Earth Sciences: A comprehensive approach to remote sensing, climate science and geosciences. *John Wiley & Sons*, (2021).
Cian, F., *et al.* Normalized Difference Flood Index for rapid flood mapping: Taking advantage of EO big data. *Remote Sensing of Environment*, vol. 209, pp. 712-730 (2018).
Clement, M.A., *et al*. Multi-temporal synthetic aperture radar flood mapping using change detection. J Flood Risk Management, 11: 152-168 (2018).
Guo, Z., *et al*. Data-driven rapid flood prediction mapping with catchment generalizability. Journal of Hydrology, vol. 609, 127726 (2022).
Hamidi, E., *et al*. Fast Flood Extent Monitoring With SAR Change Detection Using Google Earth Engine. *IEEE Transactions on Geoscience and Remote Sensing*, vol. 61, pp. 1-19, 2023, Art no. 4201419.
Hamidi, E., *et al*. Replication data for: Fast flood extent monitoring with SAR change detection using Google Earth engine, *Harvard Dataverse*, Jan. 2023.
Ireland, G., *et al.* Examining the capability of supervised machine learning classifiers in extracting flooded areas from Landsat TM imagery: a case study from a Mediterranean flood. *Remote sensing* 7.3, 3372-3399 (2015).
Long, S., *et al.* Flood extent mapping for Namibia using change detection and thresholding with SAR. Environmental research Letters, vol. 9, no.(3, art. no. 035002 (2014).
Löwe, R., *et al.* U-FLOOD – Topographic deep learning for predicting urban pluvial flood water depth. *Journal of Hydrology*, vol. 603, Part A, 126898 (2021).
Mateo-Garcia, G., *et al.* Towards global flood mapping onboard low cost satellites with machine learning. *Sci Rep* 11, 7249 (2021).
Portalés-Julià, E., *et al.* Global flood extent segmentation in optical satellite images. *Sci Rep* 13, 20316 (2023).
Vanakama, V. S. K., *et al*. Change detection based flood mapping using multi-temporal Earth Observation satellite images: 2018 flood event of Kerala, India. *European Journal of Remote Sensing*, vol. 54, no.1 pp 42-58 (2021).
Woznicki, S. A., *et al.* Development of a spatially complete floodplain map of the conterminous United States using random forest. *Science of The Total Environment* vol. 647, pp. 942-953 (2019).